

Neuronavigated Focalized Transcranial Direct Current Stimulation Administered During Functional Magnetic Resonance Imaging

Filip Niemann^{*,1}, Alireza Shababaie^{*,1}, Sven Paßmann¹, Steffen Riemann¹, Robert Malinowski¹, Harund Kocataş¹, Leonardo M. Caisachana Guevara^{1,2}, Mohamed Abdelmotaleb¹, Daria Antonenko¹, Felix Blankenburg^{3,4}, Rico Fischer², Gesa Hartwigsen^{5,6}, Shu-Chen Li^{7,8}, Michael A. Nitsche^{9,10,11}, Axel Thielscher^{12,13}, Dagmar Timmann¹⁴, Anna Fromm¹, Dayana Hayek¹, Ann-Kathrin Hubert¹, Andrew K. Martin^{15,16}, Alexander Hunold¹⁷, Agnes Flöel^{*,1,18}, Marcus Meinzer^{*,1}

¹ Department of Neurology, University Medicine Greifswald ² Department of Psychology, University Medicine Greifswald ³ Berlin School of Mind and Brain, Humboldt Universität zu Berlin ⁴ Neurocomputation and Neuroimaging Unit, Freie Universität Berlin ⁵ Wilhelm-Wundt-Institute for Psychology, Cognitive and Biological Psychology, Leipzig University ⁶ Lise Meitner Research Group Cognition and Plasticity, Max Planck Institute for Human Cognitive and Brain Sciences ⁷ Lifespan Developmental Neuroscience, Faculty of Psychology, Technische Universität Dresden ⁸ Centre for Tactile Internet with Human-in-the-Loop, Technische Universität Dresden ⁹ Department of Psychology and Neurosciences, Leibniz Research Centre for Working Environment and Human Factors ¹⁰ German Centre for Mental Health (DZPG) ¹¹ Clinic of Psychiatry and Psychotherapy, Protestant Hospital of Bethel Foundation, University Hospital OWL, Bielefeld University ¹² Danish Research Centre for Magnetic Resonance, Centre for Functional and Diagnostic Imaging and Research, Copenhagen University Hospital Amager and Hvidovre ¹³ Department of Health Technology, Technical University of Denmark ¹⁴ Department of Neurology and Center for Translational Neuro- and Behavioral Sciences (C-TNBS), Essen University Hospital ¹⁵ Department of Psychology, University of Kent ¹⁶ Kent Medway Medical School ¹⁷ Institute of Biomedical Engineering and Informatics, Technische Universität Ilmenau ¹⁸ German Center for Neurodegenerative Diseases (DZNE Site Greifswald)

* These authors contributed equally

Corresponding Authors

Filip Niemann

filip.niemann@med.uni-greifswald.de

Alireza Shababaie

Alireza.Shahbabaie@med.uni-greifswald.de

Citation

Niemann, F., Shababaie, A.,
Paßmann, S., Riemann, S.,
Malinowski, R., Kocataş, H., Caisachana
Guevara, L.M., Abdelmotaleb, M.,
Antonenko, D., Blankenburg, F.,
Fischer, R., Hartwigsen, G., Li, S.C.,
Nitsche, M.A., Thielscher, A.,
Timmann, D., Fromm, A., Hayek, D.,
Hubert, A.K., Martin, A.K., Hunold, A.,
Flöel, A., Meinzer, M. Neuronavigated
Focalized Transcranial Direct Current
Stimulation Administered During
Functional Magnetic Resonance
Imaging. *J. Vis. Exp.* (), e67155,
doi:10.3791/67155 (2024).

Abstract

Transcranial direct current stimulation (tDCS) is a noninvasive brain stimulation technique that allows the modulation of the excitability and plasticity of the human brain. Focalized tDCS setups use specific electrode arrangements to constrain the current flow to circumscribed brain regions. However, the effectiveness of focalized tDCS can be compromised by electrode positioning errors on the scalp, resulting in significant reductions of the current dose reaching the target brain regions for tDCS. Electrode placement guided by neuronavigation based on the individual's head and brain anatomy derived from structural magnetic resonance imaging (MRI) data may be suited to improve positioning accuracy.

This protocol describes the method of neuronavigated electrode placement for a focalized tDCS setup, which is suitable for concurrent administration during functional MRI (fMRI). We also quantify the accuracy of electrode placement and investigate electrode drift in a concurrent tDCS-fMRI experiment. Critical steps involve the optimization of electrode positions based on current modeling that considers the individual's head and brain anatomy, the implementation of neuronavigated electrode

Date Published

August 29, 2024

DOI

10.3791/67155

URL

jove.com/t/67155

placement on the scalp, and the administration of optimized and focal tDCS during fMRI.

The regional precision of electrode placement is quantified using the Euclidean norm (L_2 norm) to determine deviations of the actual from the intended electrode positions during a concurrent tDCS-fMRI study. Any potential displacement of electrodes (drift) during the experiment is investigated by comparing actual electrode positions before and after the fMRI acquisition. In addition, we directly compare the placement accuracy of neuronavigated tDCS to that achieved by a scalp-based targeting approach (an Electroencephalography (EEG) 10-20 system). These analyses demonstrate superior placement accuracy for neuronavigation compared to scalp-based electrode placement and negligible electrode drift across a 20 min scanning period.

Introduction

Transcranial direct current stimulation (tDCS) is a noninvasive brain stimulation technique that allows the modification of cognition and physiological brain functions in experimental and clinical contexts^{1,2,3}. Acute administration of tDCS can have transient changes in neuronal excitability, with the aftereffects lasting from minutes to hours after the stimulation^{4,5}. The applied current does not induce action potentials but rather transiently shifts the resting membrane potential of the neuron toward either de- or hyperpolarization, resulting in either increased or decreased neuronal excitability at the macroscopic level using standard protocols^{4,5,6}. Furthermore, regarding synaptic plasticity effects of tDCS, animal and human studies have shown that tDCS induces long-term potentiation and depression (LTP and LTD)-like processes^{4,5}.

In the motor system, the modulation of motor evoked potentials (MEPs) allows direct assessment of neurophysiological effects of tDCS on local cortical excitability⁷. However, this approach cannot quantify the neural effects of tDCS on higher-order cognitive functions

supported by large-scale functional brain networks⁸. The effects on brain networks can be investigated by combining tDCS with modern functional imaging techniques^{9,10}. Among those, functional magnetic resonance imaging (fMRI) has become the most frequently used approach because it provides excellent spatial and sufficient temporal resolution to reveal the neural mechanisms by which tDCS affects local brain activity at the stimulation site and large-scale neural networks^{11,12,13,14}.

So far, combined fMRI-tDCS studies have mainly employed so-called conventional tDCS setups, which use relatively large rubber electrodes between 25 and 35 cm² (5 x 5 cm² and 5 x 7 cm²) inserted into saline-soaked sponge pockets^{15,16}. These setups project the current between two electrodes that are typically attached over (a) a target brain region for tDCS and (b) a return electrode over non-target brain regions or extracranial areas (e.g., the shoulder). This results in widespread current flow across the brain, affecting regions other than the target region, thereby complicating

causal assumptions and interpretations about the neural origin of tDCS effects¹⁷.

More precise spatial targeting can be achieved by focalized tDCS¹⁸. These setups employ arrays of smaller electrodes arranged in close proximity to each other or by using a ring-shaped cathode placed around a center anode to constrain current flow to the target region^{18,19}. Computer simulations of electric current flow suggest that focalized tDCS can result in higher spatial precision of the current flow to the target region than conventional montages²⁰. Moreover, behavioral studies have demonstrated regional and task-specific behavioral modulation using focalized setups^{19,21,22}. However, only a few studies have used focalized tDCS during fMRI. These studies have been able to establish the feasibility of this approach and provided the first evidence for region-specific neural modulation^{19,23}.

However, because of regionally precise current delivery, focalized tDCS setups may be more sensitive to electrode positioning errors on the scalp than conventional montages. For example, Seo et al. demonstrated that positioning errors of 5 mm in a focalized motor cortex setup reduced peak somatic polarization in the hand knob by up to 87%²⁴. Moreover, a recent computational modeling study demonstrated that electrode displacement from intended positions for focal compared to conventional setups resulted in significant current dose reductions in the target regions for tDCS, ranging from 26% to 43%²⁵. Therefore, it was concluded that future studies should routinely include appropriate methods for the improvement of electrode positioning and the verification of electrode positioning before and after fMRI⁵.

In the present study, we describe the method of neuronavigated electrode positioning for a novel fMRI-

compatible focal 3 x 1 tDCS setup (i.e., three individual cathodes that are arranged in a circle around a single center anode), which is currently being used in a collaborative research consortium funded by the German Science Foundation (DFG Research Unit 5429, <https://www.memoslap.de>). The consortium investigates behavioral and neural effects of focalized tDCS on learning and memory and predictors of stimulation response across four functional domains (i.e., visual-spatial, language, motor, and executive functions). Structural T1- and T2-weighted MRI data of study participants are acquired during a baseline scan. These data are used for individualized current flow simulations²⁶ to determine scalp positions of electrodes that maximize the current flow to the target region in individual study participants. As an example, this protocol will describe neuronavigated targeting of individually determined electrode positions centered over the right dorsolateral prefrontal cortex (rDLPFC) in one participant.

The representative results section is based on structural imaging data acquired before and after concurrent tDCS-fMRI in three subprojects of the Research Unit. These studies targeted the right occipitotemporal cortex (rOTC), left temporo-parietal cortex (ITPC), and rDLPFC. Data were acquired at the Department of Neurology of the University Medicine Greifswald. Using these data, we aimed to achieve two main objectives: (1) To quantify the spatial precision of neuronavigated electrode placement by comparing "intended" versus empirically determined "actual" electrode positions²⁵, and (2) investigate the degree of electrode displacement over the course of the fMRI sessions (i.e., electrode drift). These factors are crucial for improving the accuracy and reliability of tDCS effects in concurrent tDCS-fMRI studies²⁷. In addition, the targeting accuracy of neuronavigated tDCS is compared to that of a scalp-based

approach using data from a previous tDCS-fMRI study of our group²⁵.

Protocol

All experimental procedures presented in this protocol have been reviewed and approved by the ethics committee of the University Medicine Greifswald. All participants provided informed consent prior to study inclusion and granted permission for their data to be published anonymously.

1. Screening of contraindications and general considerations

1. Prior to study inclusion, carefully screen participants for MRI²⁸ and tDCS²⁹ contraindications (e.g., pacemakers, claustrophobia, history of seizures, migraine, skin disease on the scalp [e.g., psoriasis/ eczema]) using appropriate questionnaires.
2. Explain the study goals and all planned procedures to the participants and obtain written informed consent according to the local requirements.
3. Follow general procedures for improving reporting and reproducibility of concurrent tDCS-fMRI experiments and test for potential imaging artifacts induced by the current and/or tDCS equipment as recommended by current guidelines³⁰.
4. Use appropriate methods to assess participant and investigator blinding^{31,32} and potential adverse effects of tDCS²⁹.

2. Baseline MRI scan and individualized current modeling

1. After completing safety checks (i.e., removal of magnetic objects from the participant, such as coins, necklaces,

piercings, etc.), guide the participant into the scanner room and position her/him comfortably on the MRI examination table. Attach the upper part of the head coil and move the participant inside the bore of the MRI scanner according to the manufacturer's specifications.

NOTE: We used a 3T scanner equipped with a 64-channel head/neck shim coil.

2. Register the new participant using the scanner interface by clicking **Main Menu | Examination | Patient Registration** and fill in the required fields. Go to **Program Choice** and collect and select the planned imaging protocol. Click on **Patient orientation** and select the **head first, Supine position** option. From the **Region of examination and laterality** dropdown menu, choose **brain** and then click **Examination** to get to the examination menu.
3. Follow the onscreen instructions of the predefined scan protocol (like adjusting the field of view, etc.) to acquire T1- and T2-weighted MRI sequences. Interact with the participant via the scanner intern communication system if necessary.
NOTE: T1- and T2-weighted images are required for individualized current modeling. The T1-weighted image is also required for neuronavigation to identify the planned and optimized positions of electrodes on the participants' scalp.
4. Use the script in <https://github.com/memoslap/Greifswald> and the structural imaging data acquired during the baseline MRI scan to conduct individualized current modeling (e.g., using SimNIBS²⁶). Follow the steps in the Readme.md file to apply the finite element method and individualized tetrahedral head meshes generated from the participant's structural T1- and T2-

weighted images (<http://simnibs.org>)^{26,33,34} **CHARM** tool³⁵ for head reconstruction to determine the peak **e-field** to determine optimized target positions for placement of tDCS electrodes over the rDLPFC. See **Figure 1** for an example of the outcome of the procedure used for this protocol.

NOTE: Alternative methods for identification of scalp coordinates for neuronavigated targeting are possible and depend on study-specific procedures.

3. Neuronavigation

1. Preparatory steps

1. Turn on the Neuronavigation control computer and the tracking system.

2. Assembly steps

1. Assemble all the required equipment for neuronavigation (**Figure 2**; for an overview of the neuronavigation setup, see **Supplemental Figure S1**). The equipment in **Figure 2** consists of (1) a subject tracker, (2) screwdriver, (3) hexagonal rod, (4) goggles, and (5) pointer. Follow the instructions below to complete the assembly.

1. Loosen the screw under the subject tracker with the screwdriver.
2. Insert the longer side of the hexagonal rod into the nut mounted on the subject tracker and tighten the screw.
3. Loosen the screw on the left side of the goggles (with the goggles positioned as if looking through them).

4. Insert the opposite side of the hexagonal rod into the nut mounted on the left side of the goggles and tighten the screw of the goggles.

NOTE: You have the option to install the subject tracker on the left or right side of the goggles. This choice depends on the target area relative to the position of the camera of the neuronavigation system (which must recognize the pointer and the subject tracker) in relation to the participant's position. In the present example, the tracker is attached on the left side so that the person conducting the tracking is not standing in between the tracker and the camera.

3. Transfer the structural T1-weighted (e.g., as a Neuroimaging Informatics Technology Initiative (NIfTI) file) of the respective participant obtained in step 2.3. to the control computer of the neuronavigation system.
4. Open the neuronavigation software and choose **New Empty Project**.
5. Load the T1-weighted image of the participant and save the project by selecting **save project**.
6. To initiate the 3D head reconstruction, go to the **Reconstructions** section in the main window of the application. Click on **New... | Skin**, which will open another window. Reconstruct the skin by pressing the respective button. Adjust the skin/air threshold if distortions are observed in the head reconstruction.

NOTE: It is suggested to check if the entire head is correctly reconstructed. A good reconstruction of the

nose and ears is important to detect the landmarks described in the next step.

7. Configure five landmarks: nasion, left and right nostrils, and left and right preauricular pits (LPA and RPA). These are required to register the participant in the **Landmarks** section of the main window of the application (for details, see **Supplemental Figure S2**).

8. Configure the electrode positions for the rDLPFC in the **Targets** section by inserting the x, y, and z coordinates of the anode position (provided by the individualized current flow simulations described in step 2.4), click on **Add new**, and type the corresponding name of the Anode. Repeat the procedure for the three return electrodes.

2. Neuronavigated identification of electrode positions

1. Position the participant comfortably in a chair facing the tracking camera. Ask him/her to put on the goggles with the subject tracker attached.
2. Instruct the participants not to touch the goggles during the entire neuronavigation procedure. This is crucial for a precise registration of the landmarks and validation of the stimulation target region.
3. Go to the **Sessions** tab, and from the left corner, choose **Online Session** from the **New** dropdown menu. Select the **Polaris** tab and verify the visibility of the subject tracker and the pointer by moving them into the camera field of view. Both devices are correctly recognized when the corresponding red crosses change to the green check marks in the **Tools** panel (left side of the application window).
4. Select the **Registration** section to register the five predefined landmarks. Find the respective landmark

by placing the pointer perpendicularly to the skull with the sensors pointing to the camera. Then, press the foot pedal of the neuronavigation system to confirm the position. Ensure that a green checkmark is seen in front of the name of each landmark.

5. Navigate to the **validation** section and validate the landmarks by placing the tip of the pointer on the registered landmarks and check the two **distance indices**; the first index shows the distance between the crosshair (virtual pointer tip) and the registered landmark, the second index shows the distance between the crosshair and the reconstructed skin.

NOTE: When using the default parameters of the neuronavigation system, indices below 5 mm indicate sufficient precision to pass the validation step. This is acceptable for many experimental contexts. However, because of the optimized focal setup used in this protocol, the validation of electrodes is only accepted if the deviation from the intended coordinates is less than 1 mm (see **Figure 3**).

6. Move the pointer over the participant's scalp and check the crosshairs of the reconstructed scalp on the neuronavigation monitor. If the crosshairs remain aligned with the reconstructed scalp without penetrating it or creating a gap above it, it is acceptable, although not recommended, to skip the next step.
7. Sample additional points around extreme point locations, including the left-most, right-most, top-most, back-most, and front-most locations on the scalp and the actual electrode positions to refine their location. To do so, click the Add button in the refinement landmarks panel for each position. Next,

position the pointer on the target surface of the head, ensuring the tip of the pointer gently touches the scalp, and press the pedal to register the position. Repeat this process until the distance between the crosshair and the reconstructed skin is as low as possible.

NOTE: Different neuronavigation systems may use different terminology to refer to this process (e.g., **surface registration**).

8. Select the **Perform** section and move the pointer to the approximate location of the DLPFC to find the position of the center anode (based on the coordinates provided in **Figure 1D**). While moving the pointer, observe the screen simultaneously. Mark the positions of the electrodes when the tip of the pointer aligns with the center of the green crosshair on the screen.
 9. Move the participant's hair away from the corresponding area on the scalp and mark the positions with a skin marker/pen. Repeat the process for the positions of the three cathodes (see **Figure 1D**).
 10. Apply a small amount of topical anesthetic cream at the intended positions of the electrodes to reduce the physical sensations on the scalp during tDCS-fMRI.
- NOTE:** Allow at least 20 min between the application of the cream and starting the tDCS.

4. tDCS-fMRI

1. Preparation for concurrent tDCS-fMRI

1. Prepare focal 3 x 1 tDCS with a multi-channel direct current (DC) stimulator.

2. Use the multi-channel DC stimulator³⁶ in **normal (non-battery) mode**. Insert the power plug of the stimulator into the same power strip as the scanner for enhanced signal-to-noise ratio and reduction of imaging artifacts (see also notes from the manufacturer's specifications).

3. Make sure all necessary stimulation-related materials are available and clean (**Figure 4**). Take special care that the rubber electrodes and 3D templates do not contain any paste from previous experimental sessions.

NOTE: The setup used in this project employs customized electrodes and filter boxes developed in collaboration with the manufacturer of the DC stimulator to meet the specific requirements of the Research Unit (see **Figure 4A**). However, standard MRI-compatible components can also be used.

1. Use a 3D-printed (thermoplastic) electrode paste fill aid to standardize the application of conductive electrode paste prior to attaching the electrodes to the scalp (**Figure 4A (9),B**).
2. Use a 3D-printed (thermoplastic) spacer to position the electrodes on the scalp and ensure that the distances between the anodes and the cathodes are maintained during the fMRI-tDCS sessions (**Figure 4A (10),C**).

NOTE: The 3D customized templates can be accessed using the following link: <https://github.com/memoslap/Material.git>

4. To set up the DC stimulator, connect the DC stimulator to the outer box (by using the outer box cable and adapter). Connect the inner box cable to the inner and outer box (see **Figure 4**).

5. Apply 1 mm of conductive gel only on the surface of all electrodes of the focal-tDCS 3x1 setup. Use the electrode fill aid to standardize the gel thickness. Cover only the surface of the electrode with the paste and remove any additional paste.

6. Turn on the DC stimulator and the Panel PC (in the given order). Double-click on the **DC-Stimulator MC** icon on the desktop. Click on the **calibrate stimulator** button to calibrate the stimulator with no electric load (i.e., the participant is not connected to the stimulator).

CAUTION: If the participant is connected to the stimulator while calibrating, the electric current can induce painful sensations.

7. Position the participant comfortably near the DC stimulator outside the MRI scanner room.

8. Determine the widest part of the participant's head, from the forehead (just above the eyebrows) to the occipital bone at the back of the head. Choose the optimal size of the EEG cap to keep the electrodes in place during the tDCS-fMRI session.

9. Place the electrodes in the spacer to ensure equal spacing of the cathodes around the center anode and attach the electrodes over the identified and marked scalp positions.

10. Use the optimal size EEG cap without plastic inserts to keep the electrodes in place during tDCS-fMRI.

NOTE: Make sure that electrodes do not get displaced while the cap is put in place.

11. Connect the leads of the electrode cables to the inner box of the DC stimulator to perform an impedance check. Select the required stimulation sequence at the **selected sequence setup**

dropdown menu. Initiate the impedance check by pressing the **impedance check** button on the DC stimulator. Make sure that **MR mode** is checked.

12. Conduct the **Impedance Check** by pressing the respective button on the stimulator interface; if the impedance is ≤ 25 k Ω , go to the next step (4.1.13). If the impedance is higher for any electrode, softly press the electrodes to the scalp, tighten the cap, and allow the conductive paste to warm up. If required, apply more paste.

13. Disconnect the inner box from the outer box and insert the outer box into the waveguide of the scanner.

14. Guide the participant into the scanner room while holding on to the inner box and connected electrode cables.

NOTE: At any time, take great care that there is no pull the cables, which could result in electrode displacement.

15. Ask the participant to sit on the MRI examination table and re-connect the inner box to the outer box (that is inserted in the waveguide of the scanner).

16. Place the participant comfortably in a supine position on the MRI examination table, with the head positioned in the open head coil. Use inflatable cushions on both sides of the head and an extra cushion at the top of the head to stabilize it.

NOTE: Inflatable cushions are preferred at the sides to foam cushions to avoid electrode displacement when the foam cushions are inserted.

17. Lead the electrode cables through the lower part of the head coil before attaching the upper part of the head coil and locking it in place.

18. Position the inner box next to the participant on the MRI examination table and move the participant into the scanner bore.

19. Leave the scanner room and inform the participant about the upcoming procedures via the communication interface of the scanner prior to each structural and functional imaging sequence, as well as prior to the second impedance check inside the scanner.

2. Concurrent tDCS-fMRI

1. On the **scanner Panel PC**, register the new participant by clicking **Main Menu | Examination | Patient Registration** and fill in the required necessary fields. Go to **Program Choice** and collect and select the planned imaging protocol. Click on **Patient orientation** and select the **head first, Supine position** option. From the **Region of examination and laterality** dropdown menu, choose **brain** and click **Examination** to get to the examination menu.

2. Follow the onscreen instructions to acquire the planned scans (pre-fMRI Pointwise Encoding Time reduction with Radial Acquisition (PETRA), fMRI, post-fMRI PETRA) in the order shown in the following steps of this protocol.

1. Acquire a **PETRA** scan that allows verification of the electrode positions on the participant's head.
2. Inform the participant that two 10 min resting-state fMRI scans will be conducted and that he/she should maintain their gaze on a fixation cross (displayed via a projector and mirrors

mounted on the head coil) for the entire duration of the scanning period (2 x 10 min).

3. Start the tDCS stimulation by pressing the **init stimulation** button on the Panel PC. Click the **release start-trigger** button to start the stimulation with a 10 s ramp-up prior to commencing with the functional imaging sequences. Administer **tDCS** for **20 min** with **2 mA**.

NOTE: Other stimulation protocols with different ramping periods or stimulation intensities or durations are possible.

4. After the end of the functional scans and stimulation period, acquire a second **PETRA** scan while the electrodes are still attached to the participant's head.

NOTE: By comparison with the pre-fMRI PETRA scan, this allows the determination of potential electrode movement across the tDCS-fMRI experiment (i.e., drift).

3. Upon completion of the MRI session, disconnect the electrode cables from the outer box and turn off the DC stimulator, move the participant out of the scanner bore, remove the cap from the participant's head, and remove the electrodes.
4. Inspect the participant's scalp for potential skin redness caused by the stimulation. Clean the participant's scalp where the electrodes were placed.
5. At the end of the experiment, ask the participant to complete the tDCS adverse effects²⁹ and blinding^{31,32} questionnaires.

Representative Results

Data from 43 healthy young participants (20 men/23 women, aged 24.74 ± 5.50 years) were included. The participants completed up to four fMRI sessions. Neuronavigated placement of electrodes was conducted prior to each fMRI session. In total, 338 datasets representing the positions of the center anodes before and after fMRI were included in data analyses.

To determine the **intended** positions of the electrodes, individualized current modeling was performed using structural MRI data acquired in a separate MRI session (prior to the fMRI sessions). Current modeling aimed to optimize scalp the positions of the 3 x 1 setups to maximize current flow to the rDLPFC (N = 19, participants/N = 137 data points), rOTC (N = 12/104) or ITPJ (N = 12/97).

Actual positions of the center anodes of the 3 x 1 setup were empirically determined using structural MRI data (PETRA images) acquired before and after each fMRI session (Note: Coordinates for targeting were provided in subject space. Hence, PETRA scans of individual participants were co-registered with their own T1-weighted image acquired during the baseline scan, on which field simulations were based). Because identification of electrode positions in 3D is prone to errors, a modified 2D "pancake" view of the reconstructed scalp with electrodes was used (see **Figure 5**^{37,38}) to determine six edge points of the center anodes. Subsequently, the center of mass was calculated to obtain the center coordinates of the anodes for each fMRI session and time-point (i.e., before or after tDCS). Subsequently, a reverse 2D->3D transformation was applied to obtain electrode coordinates in 3D space.

The spatial precision of the neuronavigated electrode placement was investigated by comparing "intended" vs "actual" electrode positions²⁵ and is reported as the L²-Norm (Euclidean norm) distance³⁹. The L²-Norm is a standard vector norm calculated as the square root of the sum of the squares of the vector components. The vector components are the differences between intended and planned coordinates for each dimension of the 3D space (x/y/z). Electrode displacement over the course of the experiment (i.e., drift) was investigated by comparing actual electrode positions determined before and after fMRI.

In addition, we compared targeting accuracy for neuronavigated electrode placement with data from a previous study of our group that used a scalp-based targeting approach (EEG-20 system²⁵). This study comprised data from 60 participants (31 men/29 women, aged 22.17 ± 2.33 years), two target regions (N = 30/30, motor cortex/inferior frontal gyrus) and two fMRI sessions for a total of 240 data points. Data and code used for all analyses are publicly available at https://github.com/LawsOfForm/VerFlu_Simulation_Niemann_2023.

Linear mixed models were used to analyze (a) deviation of actual electrode positions from intended locations and (b) drift across the fMRI session with the following formula and the L² Norm as the dependent variable:

$$y_{ij} = \beta_0 + \text{POSITION}x_{1ij} + \text{REGION}x_{2ij} + \text{POSITION} * \text{REGION}x_{3ij} + \mu_{0j} + \epsilon_{ij}$$

y_{ij} is the L² Norm distance between intended and actual electrode positions at POSITION i of subject j . β_0 is the fixed effect intercept, X_1 is the value for POSITION (1: intended, 2: actual pre-fMRI; 3: post-fMRI) at position i in subject j . X_2 is the value for the REGION of interest (1: ITPC, 2:

rDLPFC, 3:rOTC) at region i in subject j . X_3 is the value for the interaction for POSITION and REGION for position and region i and subject j , u_0 is the random intercept for subject j ($\mu_{0j} \sim N(0, \tau_{002})$); ε_{ij} are the residuals for timepoint i in subject j ($\varepsilon_{ij} \sim N(0, \sigma^2)$).

Comparison of targeting accuracy for neuronavigated and scalp-based electrode placement was done using a t -test and based on the L^2 Norm differences between the intended and actual positions in the respective groups.

Neuronavigated placement accuracy and displacement across the experiment

The reference model (intended placement of center anodes; region: ITPC) showed significant deviations of electrode positions from intended positions at both pre-fMRI and post fMRI assessments (8.71 mm, 95%-CI: [6.57-10.84], $p < .001$; 8.51 mm, 95%-CI: [6.35-10.66], $p < .001$) **Supplemental Table S1**. Post-hoc analysis for estimated marginal means (EMMs) were calculated for all main and simple effects of interest (see **Supplemental Table S2**, **Supplemental Table S3**, **Figure 6**, **Figure 7**, **Supplemental Figure S3**, and **Supplemental Figure S4**). The predicted average placement error for all pre-fMRI sessions was 8.54 mm 95%-CI: [7.66-9.42] and significantly different from the intended positions ($t(296) = -8.54$, $p < 0.0001$). This was also the case for post-fMRI coordinates (8.61 mm, 95%-CI:

[7.73-9.50]; $t(296) = -10.97$, $p < 0.0001$, see **Figure 6** and **Supplemental Table S2**). Because placement errors may vary by region^{25,40,41}, misplacement was also calculated between target regions for each position. However, no region-specific differences between rOTC, ITPC, and rDLPFC were found (**Supplemental Table S3**, **Figure 7**, and **Supplemental Figure S4**).

Displacement of center anodes (i.e., drift), assessed by comparison of actual electrode positions between pre- and post fMRI was negligible (-0.08 ± 0.39 mm; $t(291) = -0.20$, $p = 0.98$). For details, see **Figure 6** and **Supplemental Table S2**.

Comparison of electrode placement errors between neuronavigated and scalp-based placement approaches

To investigate the relevance of neuronavigated placement, L^2 Norm differences between intended and actual positions based on neuronavigated electrode placement were retrospectively compared to data obtained from a previous study that used a scalp-based targeting approach²⁵. In this study, the L^2 Norm difference between the intended and actual positions of the anode was 12.33 ± 5.67 mm. Direct comparison between neuronavigated (8.83 ± 4.68) and scalp-based approaches revealed a significant decrease of the L^2 Norm distance by 3.50 mm in favor of neuronavigated electrode placement ($t(397) = 4.91$, $p < 0.001$).

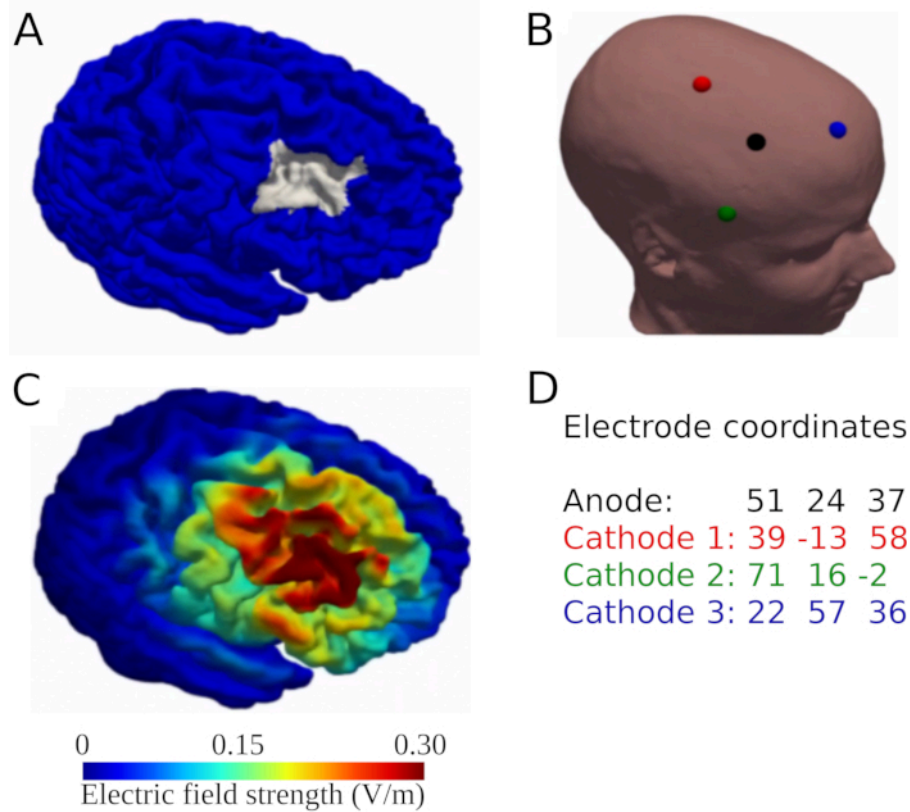


Figure 1: A simplified description of the sequence of steps representing the method for individualized current modeling. The method aims to determine optimized scalp positions of electrodes over the target region (right DLPFC) using a focal 3 x 1 tDCS setup. **(A)** Anatomical target region in gray. **(B)** Optimized electrode position illustrated on the reconstructed head of the participant (anode = black, cathode 1 = red, cathode 2 = green, cathode 3 = blue). **(C)** Simulated electric field based on individualized current modeling for this montage (in V/m). **(D)** Target coordinates for all intended electrode positions used during neuronavigated targeting (dimensions: x/y/z). Abbreviations: DLPFC = right dorsolateral prefrontal cortex; tDCS = transcranial direct current stimulation. [Please click here to view a larger version of this figure.](#)

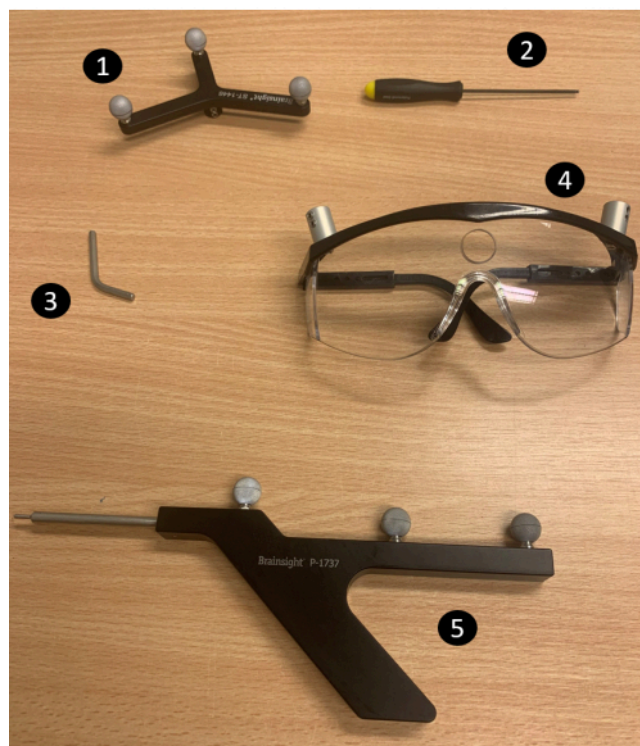


Figure 2: Neuronavigation equipment. 1) Subject tracker, 2) Screwdriver, 3) Hexagonal rod, 4) Goggles, 5)

Pointer. **NOTE:** The neuronavigation software communicates with the position sensor (the tracking camera) to obtain the location of the subject tracker (mounted on the goggles). It uses a registration matrix (obtained by identifying landmarks on the subject's head through the pointer) to align the subject's head position from the real world to the participant's image space (based on the T1-weighted image of the participant). An overview of the overall setup is provided in **Supplemental Figure S1**. [Please click here to view a larger version of this figure.](#)

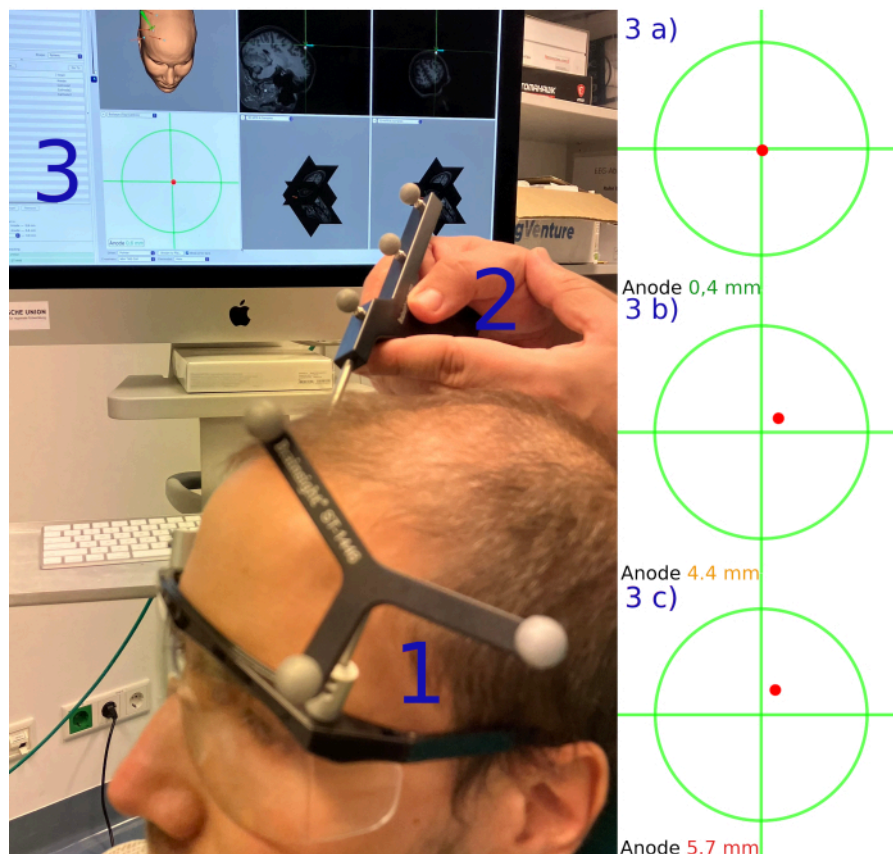


Figure 3: Target region validation. Illustrates the procedure of validating stimulation target regions via neuronavigation.

1) The Subject tracker assembled on the left side of goggles. 2) The Pointer is used to locate the intended position of the anode (rDLPFC). 3) The green crosshair and the red dot (representing the tip of the pointer) on the computer screen. 3a) The index number is green if the pointer deviates from the crosshair by less than 3 mm; 3b) the index number is orange if the pointer deviates between 3 and 5 mm; and 3c) it is red if the pointer deviates more than 5 mm. Abbreviation: rDLPFC = right Dorsolateral Prefrontal Cortex. [Please click here to view a larger version of this figure.](#)

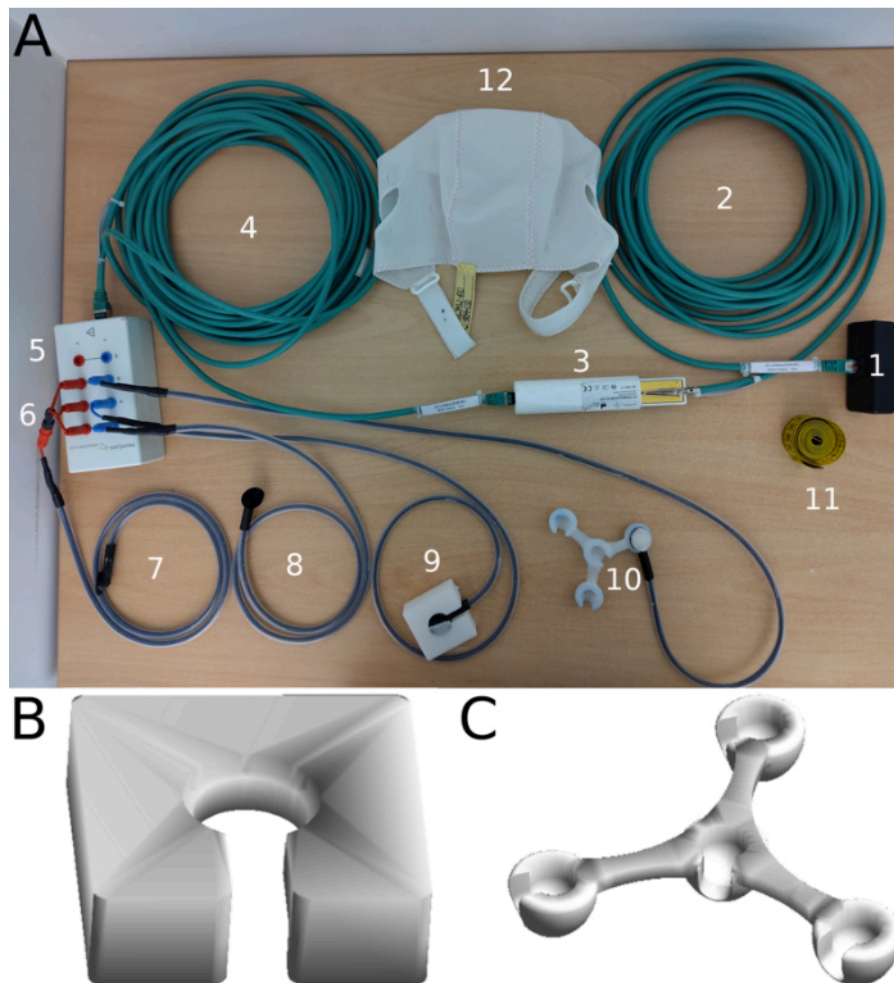


Figure 4: Selected components of multi-channel DC-stimulator and *custom components. (A) 1) Adapter that plugs into the DC stimulator outlet, 2) Outer box LAN cable, 3) *Outer box (filter box) that is positioned inside the waveguide of the scanner during tDCS-fMRI. The clamp is attached to the waveguide to connect the filter box with the floating mass of the shielded MRI chamber to reduce potential artifacts. 4) Inner box cable, 5) inner box with plugs for electrode cables, 6) *fuse adapter that combines three individual channels to one for the center anode, 7) *fused electrode cables and electrode of the center anode (10 mm radius) made of flexible and electrically conductive silicone, 8) individual cathode and cable, 9) example of electrode inserted into 3D printed fill aid, 10) example of electrode placed in 3D spacer, 11) measuring tape, 12) EEG cap without plastic inserts to secure electrodes on the scalp. For the complete setup and standard components not used in this protocol, readers are referred to the website of the manufacturer (link in **Table of Materials**). (B) 3D model of the electrode fill aid. (C) 3D model of the spacer. Abbreviations: tDCS-fMRI = transcranial direct current stimulation-functional magnetic resonance imaging; EEG = electroencephalography. [Please click here to view a larger version of this figure.](#)

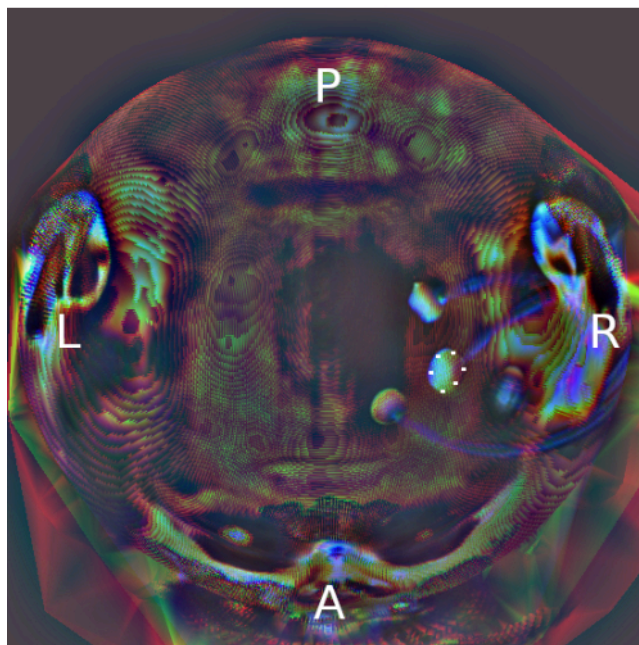


Figure 5: Pancake view of scalp and electrodes based on the PETRA image. Colors represent different sizes of scalp flattened mask (red = 2 mm; green = 4 mm, blue = 6 mm of the inflated scalp for depth visualization of the head). Orientations of the transformed image are marked in white letters. White dots represent manually selected edge points of the center anode placed over the right dorsolateral prefrontal cortex. The center of mass was calculated as the midpoint coordinate of the edge points prior to retransformation into 3D space. Abbreviations: PETRA = Pointwise Encoding Time reduction with Radial Acquisition; L = left; R = right; P = posterior; A = anterior. [Please click here to view a larger version of this figure.](#)

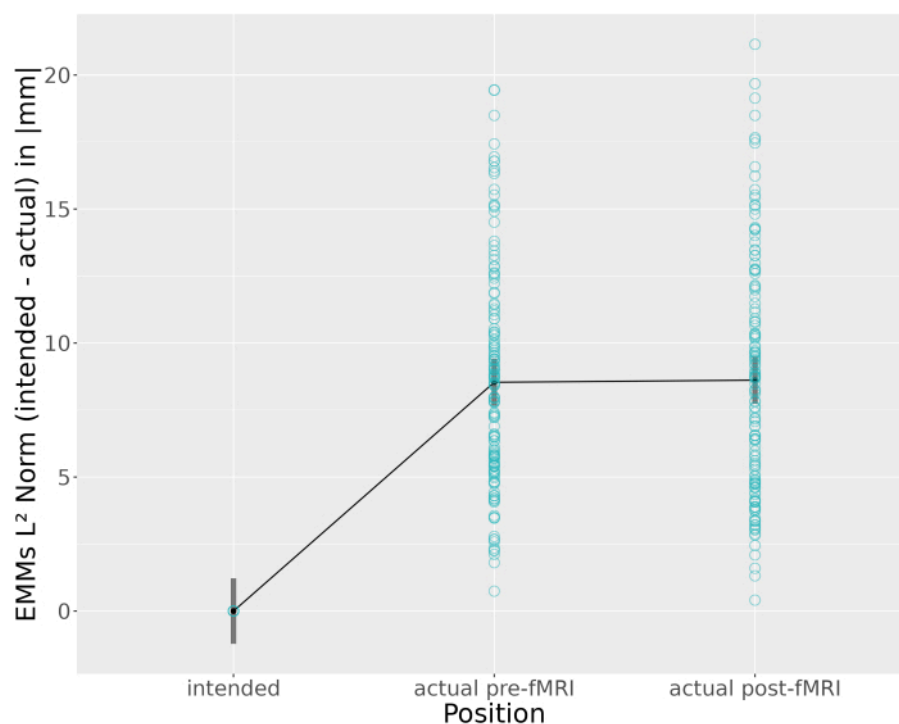


Figure 6: Estimated Marginal Means of the L^2 Norm (Euclidean norm) distance between intended and actual electrode positions of the anodal electrode across all sessions and regions (rOTC, ITPC, rDLPFC). Original data points in turquoise. EMMs 95% confidence intervals in grey. Abbreviations: EMMs = Estimated Marginal Means; rOTC = Right Occipital Temporal Cortex; ITPC = left Temporal Parietal Cortex; rDLPFC = right Dorsolateral Prefrontal Cortex; fMRI = functional magnetic resonance imaging. [Please click here to view a larger version of this figure.](#)

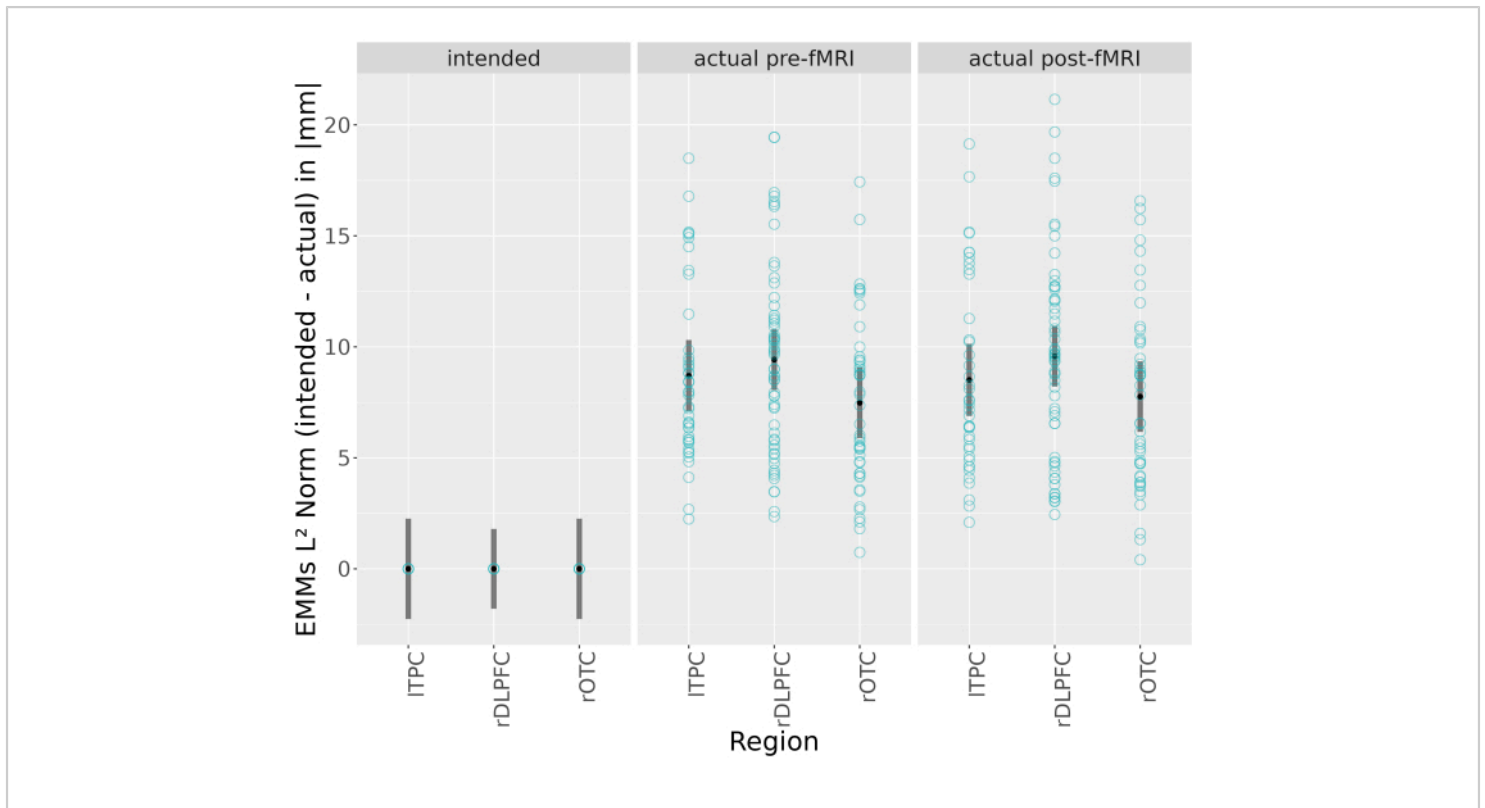


Figure 7: Estimated Marginal Means of L^2 Norm (Euclidean norm) distance between intended and actual electrode positions of the anodal electrode over all sessions between each region (rOTC, ITPC, rDLPFC) for each position (intended, pre/post fMRI). Original data points in turquoise. EMMs 95% confidence intervals in grey. Abbreviations: EMMs = Estimated Marginal Means; rOTC = Right Occipital Temporal Cortex; ITPC = left Temporal Parietal Cortex; rDLPFC = right Dorsolateral Prefrontal Cortex; fMRI = functional magnetic resonance imaging. [Please click here to view a larger version of this figure.](#)

Supplemental Figure S1: The neuronavigation system overview. 1) Control computer of the neuronavigation system with the neuronavigation software installed; 2) Polaris camera; 3) Foot pedal; 4) Goggles with subject tracker (see **Figure 2** for details); 5) Pointer. [Please click here to download this File.](#)

Supplemental Figure S2: Reconstructed skin with landmarks in yellow. 1) Nasion, 2) left nostril; 3) right nostril; 4) left preauricular pit; 5) right preauricular pit (see protocol

step 3.1.7). Abbreviations: LPA = left preauricular pit; RPA = right preauricular pit. [Please click here to download this File.](#)

Supplemental Figure S3: Estimated Marginal Means of L^2 Norm (Euclidean norm) distance between intended and actual electrode positions of the anodal electrode across all sessions between positions (intended, pre/post fMRI) for each region (rOTC, ITPC, rDLPFC). Original data points in turquoise. EMMs 95% confidence intervals in grey. Abbreviations: EMMs = Estimated Marginal Means; rOTC = Right Occipital Temporal Cortex; ITPC = left Temporal

Parietal Cortex; rDLPFC = right Dorsolateral Prefrontal Cortex; fMRI = functional magnetic resonance imaging.

[Please click here to download this File.](#)

Supplemental Figure S4: Estimated Marginal Means of L^2 Norm (Euclidean norm) distance between intended and actual electrode positions of the anodal electrode across all sessions and positions (intended, pre/post fMRI) for each region of interest (rOTC, ITPC, rDLPFC). Original data points in turquoise. EMMs 95% confidence intervals in grey. Right Occipital Temporal Cortex (rOTC), left Temporal Parietal Cortex (ITPC), right Dorsolateral Prefrontal Cortex (rDLPFC). [Please click here to download this File.](#)

Supplemental Table S1: Results of linear mixed model analysis for L^2 Norm (Euclidian norm) distance between intended and actual coordinates. Regression coefficients of linear mixed models (random intercept models) and two-sided p-values are reported. Abbreviations: CI = confidence interval; rOTC = Right Occipital Temporal Cortex; ITPC = left Temporal Parietal Cortex; rDLPFC = right Dorsolateral Prefrontal Cortex; df = degrees of freedom; σ^2 = pooled residual variance; τ = pooled variance explained by subjects; ICC = Intraclass correlation coefficient; N = number of subjects. [Please click here to download this File.](#)

Supplemental Table S2: Post-hoc EMMs for Linear Mixed Model analysis for L^2 Norm (Euclidian norm) differences). Main and simple contrasts for main effect of position (intended, pre/post fMRI, see also **Supplemental Figure S2**) and simple effects of position for each region (ITPC, rDLPFC, rOTC, see also **Figure 6**). For simple effects, only significant effects are shown. Abbreviations: EMMs = Estimated Marginal Means; SE = Standard Error; df = degrees of freedom; rOTC = right Occipital Temporal Cortex; ITPC =

left Temporal Parietal Cortex; rDLPFC = right Dorsolateral Prefrontal Cortex. [Please click here to download this File.](#)

Supplemental Table S3: Post-hoc EMMs for Linear Mixed Model analysis of L^2 Norm (Euclidian norm) difference.

Main and simple contrasts for main effect of region (ITPC, rDLPFC, rOTC, see also **Supplemental Figure S3**) and simple effects of region for each position (intended, pre/post fMRI, see also **Figure 7**). Abbreviations: EMMs = Estimated Marginal Means; SE = Standard Error; df = degrees of freedom; rOTC = right Occipital Temporal Cortex; ITPC = left Temporal Parietal Cortex; rDLPFC = right Dorsolateral Prefrontal Cortex. [Please click here to download this File.](#)

Discussion

Critical steps, potential modifications, and troubleshooting of the method

Accurate positioning of electrodes is a crucial technical factor in tDCS experiments, and deviations from intended scalp positions or electrode drift can affect current flow to the intended target brain regions^{42,43}. This is particularly relevant for focalized tDCS, as the regional specificity of the administered current makes these setups particularly susceptible to the effects of positioning errors^{5,25}. In the current protocol, we described a method of neuronavigated, focalized tDCS administered during fMRI, which aims to enhance the placement accuracy of individually determined scalp positions. Critical steps include (1) the use of electrical current flow modeling to optimize scalp position of the 3 x 1 setup for each study participant, (2) identification of optimized scalp positions by neuronavigation, (3) positioning and securing of electrodes on the scalp using standardized procedures, and (4) investigation of placement accuracy and electrode drift before and after concurrent tDCS-fMRI.

The first step in our protocol describes the optimization of electrode positions for an individual study participant of our ongoing Research Unit (RU) by means of individualized current modeling (code to rebuild the optimization can be found here <https://github.com/memoslap/Greifswald>). This approach is highly specific to the RU projects and involved two preparatory steps not reported here: (1) Definition of anatomical target regions for eight empirical RU projects (www.memoslap.de) based on fMRI and/or tDCS studies that used the same/similar motor or cognitive tasks; (2) equalizing the average current dose across projects by adjusting the spacing between the center anode and the surrounding cathodes. This involved a computational modeling study and structural imaging data available to our group to determine the project-specific spacing of electrodes. These project-specific montages were then used to optimize scalp positions for individual participants in the RU projects to achieve maximal current intensity in the respective target regions (in this protocol: right DLPFC). Notably, there are many possible ways to determine the desired scalp positions, and those depend on the goals of the study (i.e., regional or dose control, anatomical or functional targeting).

Similarly, there are a number of different commercially available neuronavigation devices and DC stimulators that can be used for neuronavigated placement and conducting a tDCS-fMRI study. Consequently, modifications of the procedures outlined in this protocol will be required if equipment from different manufacturers is used or tDCS-fMRI is conducted with a different scanner type. Nonetheless, we believe that the protocol can be adapted in a flexible way to meet study-specific requirements. For example, for 3 x 1 setups, we recommend using a 3D printed spacer to ensure that the desired distance between the electrodes is achieved and maintained during placement and scanning.

Standardization of the amount of conductive paste can be achieved using an electrode fill aid as described in this protocol. To allow for customization, the 3D models used for printing have been made publicly available (see protocol step 4.1.3.2).

The complexity of intrascanner tDCS fMRI experiments is another crucial consideration, which requires participants to move into electrodes attached to their heads. These studies carry a significant risk of subsequent electrode displacement, even with precise positioning⁵. Therefore, we recommend routinely implementing appropriate methods to minimize electrode displacement and drift (e.g., using standard MRI-compatible inflatable cushions to avoid displacement of electrodes inside the MRI scanner, EEG caps or contoured straps to keep electrodes in place, and other measures detailed in the protocol above).

Finally, compared to behavioral tDCS studies, administering tDCS during fMRI allows for the verification of the exact positions of electrodes on the scalp (based on 3D structural MRI images) and the quantification of potential deviations from the intended positions. However, the identification of electrode positions in 3D is prone to errors. Therefore, we suggest a 2D transformation of the scalp and electrodes to facilitate the verification of actual electrode positions. However, future studies are required to validate this novel approach and compare outcomes to data extraction from 3D images.

Significance of method relative to existing other methods

Scale-based targeting approaches (e.g., the EEG-10-20 system¹⁴) have been used in the majority of tDCS research to date. This involves manual or automated identification of anatomical landmarks and additional measurements (e.g., head circumference, calculation of intersections between

landmarks) to determine the intended scalp positions of the electrodes. While this approach accounts for the head size of individual participants to some extent, it neglects other characteristics of brain and skull morphology, resulting in a loss of accuracy^{5,41,45}. The enhanced precision that can be achieved with MRI-guided neuronavigation is illustrated in the representative results section of this protocol. Here, we quantified the precision of neuronavigated targeting using data from an ongoing multicenter tDCS-fMRI study and retrospectively compared placement accuracy of neuronavigated targeting with a scalp-based approach. In addition, we investigated the degree of electrode displacement during fMRI. The main outcomes of the empirical part of this protocol were that (1) neuronavigated targeting is superior to scalp-based electrode placement, with approximately 40% higher precision based on the L^2 Norm; and (2) there was minimal drift of electrodes across fMRI sessions, highlighting that the implemented technical and procedural steps to keep electrodes in place (i.e., cap, spacer, inflatable cushions) were successful.

Limitations and future applications of the method

There are several limiting factors for using the approach described in this protocol. For example, optimization of the intended electrode positions by computational modeling, neuronavigated targeting, and verification of electrodes require access to structural MRI data, specific technical expertise, and costly equipment that may not be available. Hence, this approach is limited to specialized research centers performing studies that require high spatial precision of current delivery (e.g., experimental studies in neurotypical populations investigating causal brain-behavior relationships or computational modeling studies investigating dose-response relationships). In this context, it is worth mentioning that the validity of MRI-based current modeling may be

decreased in patients with head surgery or progressive lesions, which needs to be taken into consideration when applying the methods described in this protocol to clinical populations.

In addition, the optimization of electrode positions by computational modeling and neuronavigated placement in this protocol aims to maximize anatomical precision. As mentioned above, other ways of individualized targeting are possible (including invasive approaches limited to specific clinical populations⁴⁶), and anatomical precision does not necessarily imply functional relevance of the stimulated area. The latter would require a localizer task (either on the individual participant or group level), acquired prior to tDCS-fMRI, to identify functionally relevant brain regions for neuronavigated targeting. In addition, future research needs to determine the functional relevance of electrode displacement on behavioral and neural functions, including a direct comparison of effects between focal and conventional montages.

It should be noted that computer simulations rely on the anatomical precision of the (semi-)automated tissue segmentations acquired from MRI and estimate the electric field based on assumptions about the electrical conductivity of various tissue classes^{5,47}. Therefore, to increase the accuracy of computational models, it is essential to validate these assumptions and evaluate the segmentation accuracy. In this regard, new methods to study brain tissue's tDCS-induced current flow conductivity during simultaneous tDCS-MRI measurements include Magnetic Resonance Current Density Imaging (MRCDI) and Magnetic Resonance Electrical Impedance Tomography (MREIT)^{5,48,49}. These approaches have the potential for validating tDCS electric field simulations and optimizing individualized current

dose calculations. Combining such optimized computational modeling approaches with neuronavigated tDCS will likely improve the precision and effectiveness of tDCS in experimental and clinical contexts in the near future.

Disclosures

MAN is in the scientific advisory boards of Neuroelectrics and Précis. AH is partially employed by neuroConn GmbH. The other authors have no conflicts of interest to declare.

Acknowledgments

This research was funded by the German Research Foundation (project grants: FL 379/26-1; ME 3161/3-1; CRC INST 276/741-2 and 292/155-1, Research Unit 5429/1 (467143400), FL 379/34-1, FL 379/35-1, FI 379/37-1, FI 379/22-1, FI 379/26-1, ME 3161/5-1, ME 3161/6-1, AN 1103/5-1, TH 1330/6-1, TH 1330/7-1). AT was supported by the Lundbeck Foundation (grant R313-2019-622). We thank Sophie Dabelstein and Kira Hering for their help with data extraction.

References

1. Perceval, G., Flöel, A., Meinzer, M. Can transcranial direct current stimulation counteract age-associated functional impairment? *Neurosci Biobehav Rev.* **65**, 157-172 (2016).
2. Simonsmeier, B. A., Grabner, R. H., Hein, J., Krenz, U., Schneider, M. Electrical brain stimulation (tES) improves learning more than performance: A meta-analysis. *Neurosci Biobehav Rev.* **84**, 171-181 (2018).
3. Chan, M. M. Y., Yau, S. S. Y., Han, Y. M. Y. The neurobiology of prefrontal transcranial direct current stimulation (tDCS) in promoting brain plasticity: A systematic review and meta-analyses of human and rodent studies. *Neurosci Biobehav Rev.* **125**, 392-416 (2021).
4. Stagg, C. J., Antal, A., Nitsche, M. A. Physiology of transcranial direct current stimulation. *J ECT.* **34** (3), 144-152 (2018).
5. Meinzer, M. et al. Investigating the neural mechanisms of transcranial direct current stimulation effects on human cognition: current issues and potential solutions. *Front Neurosci.* **18**, e1389651 (2024).
6. Sandrini, M., Umiltà, C., Rusconi, E. The use of transcranial magnetic stimulation in cognitive neuroscience: A new synthesis of methodological issues. *Neurosci Biobehav Rev.* **35** (3), 516-536 (2011).
7. Bashir, S. et al. Effects of anodal transcranial direct current stimulation on motor evoked potentials variability in humans. *Physiol Rep.* **7** (13), e14087 (2019).
8. Breakspear, M. Dynamic models of large-scale brain activity. *Nat Neurosci.* **20** (3), 340-352 (2017).
9. Crosson, B. et al. Functional imaging and related techniques: an introduction for rehabilitation researchers. *J Rehabil Res Dev.* **47** (2), vii-xxxiv (2010).
10. Mier, W., Mier, D. Advantages in functional imaging of the brain. *Front Hum Neurosci.* **9**, 249 (2015).
11. Antonenko, D. et al. Microstructural and functional plasticity following repeated brain stimulation during cognitive training in older adults. *Nat Commun.* **14** (1), e3184 (2023).
12. Jamil, A. et al. Current intensity- and polarity-specific online and aftereffects of transcranial direct current stimulation: An fMRI study. *Hum Brain Mapp.* **41** (6), 1644-1666 (2020).

13. Keeser, D. et al. Prefrontal transcranial direct current stimulation changes connectivity of resting-state networks during fMRI. *J Neurosci.* **31** (43), 15284-15293 (2011).
14. Meinzer, M., Lindenberg, R., Antonenko, D., Flaisch, T., Floel, A. Anodal transcranial direct current stimulation temporarily reverses age-associated cognitive decline and functional brain activity changes. *J Neurosci.* **33** (30), 12470-12478 (2013).
15. Nardo, D. et al. Transcranial direct current stimulation with functional magnetic resonance imaging: a detailed validation and operational guide. *Wellcome Open Res.* **6**, 143 (2023).
16. Meinzer, M. et al. Transcranial direct current stimulation and simultaneous functional magnetic resonance imaging. *J Vis Exp.* (86), e51730 (2014).
17. Bergmann, T. O., Hartwigsen, G. Inferring causality from noninvasive brain stimulation in cognitive neuroscience. *J Cogn Neurosci.* **33** (2), 195-225 (2021).
18. Villamar, M. F. et al. Technique and considerations in the use of 4x1 ring high-definition transcranial direct current stimulation (HD-tDCS). *J Vis Exp.* (77), e50309 (2013).
19. Gbadeyan, O., McMahon, K., Steinhauser, M., Meinzer, M. Stimulation of dorsolateral prefrontal cortex enhances adaptive cognitive control: A high-definition transcranial direct current stimulation study. *J Neurosci.* **36** (50), 12530-12536 (2016).
20. Kuo, H.-I. et al. Comparing cortical plasticity induced by conventional and high-definition 4 × 1 ring tDCS: A neurophysiological study. *Brain Stimul.* **6** (4), 644-648 (2013).
21. Martin, A. K., Su, P., Meinzer, M. Common and unique effects of HD-tDCS to the social brain across cultural groups. *Neuropsychologia.* **133**, e107170 (2019).
22. Martin, A. K., Kessler, K., Cooke, S., Huang, J., Meinzer, M. The right temporoparietal junction is causally associated with embodied perspective-taking. *J Neurosci.* **40** (15), 3089-3095 (2020).
23. Müller, D., Habel, U., Brodtkin, E. S., Clemens, B., Weidler, C. HD-tDCS induced changes in resting-state functional connectivity: Insights from EF modeling. *Brain Stimul.* **16** (6), 1722-1732 (2023).
24. Seo, H., Kim, H.-I., Jun, S. C. The effect of a transcranial channel as a skull/brain interface in high-definition transcranial direct current stimulation-a computational study. *Sci Rep.* **7** (1), e40612 (2017).
25. Niemann, F. et al. Electrode positioning errors reduce current dose for focal tDCS set-ups: Evidence from individualized electric field mapping. *Clin Neurophysiol.* **162**, 201-209 (2024).
26. Thielscher, A., Antunes, A., Saturnino, G. B. Field modeling for transcranial magnetic stimulation: A useful tool to understand the physiological effects of TMS? *2015 37th Annual International Conference of the IEEE Engineering in Medicine and Biology Society (EMBC).* 222-225 (2015).
27. Meinzer, M. et al. Investigating the neural mechanisms of transcranial direct current stimulation effects on human cognition: current issues and potential solutions. *Frontiers in Neuroscience.* **18**, 1389651 (2024).
28. Ghadimi, M., Sapra, A. Magnetic resonance imaging contraindications. *StatPearls.* (2024).

29. Antal, A. et al. Low intensity transcranial electric stimulation: Safety, ethical, legal regulatory and application guidelines. *Clin Neurophysiol.* **128** (9), 1774-1809 (2017).
30. Ekhtiari, H. et al. Transcranial direct current stimulation to modulate fMRI drug cue reactivity in methamphetamine users: A randomized clinical trial. *Hum Brain Mapp.* **43** (17), 5340-5357 (2022).
31. Dinn, W. et al. Effectiveness of tDCS blinding protocol in a sham-controlled study. *Brain Stimul.* **10** (2), 401 (2017).
32. Turner, C., Jackson, C., Learmonth, G. Is the "end-of-study guess" a valid measure of sham blinding during transcranial direct current stimulation? *Eur J Neurosci.* **53** (5), 1592-1604 (2021).
33. Saturnino, G. B. et al. SimNIBS 2.1: A comprehensive pipeline for individualized electric field modelling for transcranial brain stimulation. *Brain and Human Body Modeling.* 3-25 (2019).
34. Windhoff, M., Opitz, A., Thielscher, A. Electric field calculations in brain stimulation based on finite elements: An optimized processing pipeline for the generation and usage of accurate individual head models. *Hum Brain Mapp.* **34** (4), 923-935 (2013).
35. Puonti, O. et al. Accurate and robust whole-head segmentation from magnetic resonance images for individualized head modeling. *NeuroImage.* **219**, e117044 (2020).
36. neuroConn Programmable multichannel current stimulator -- DC-Stimulator MC Instruction for use -- (Version 5.3.1) (2021).
37. Fleury, M., Barillot, C., Mano, M., Bannier, E., Maurel, P. Automated electrodes detection during simultaneous EEG/fMRI. *Frontiers in ICT.* **5** (2019).
38. De Munck, J. C., Van Houdt, P. J., Gonçalves, S. I., Van Wegen, E., Ossenblok, P. P. W. Novel artefact removal algorithms for co-registered EEG/fMRI based on selective averaging and subtraction. *NeuroImage.* **64**, 407-415 (2013).
39. Rich, T. L. et al. Determining electrode placement for transcranial direct current stimulation: A comparison of EEG- versus TMS-guided methods. *Clin EEG Neurosci.* **48** (6), 367-375 (2017).
40. Okamoto, M. et al. Three-dimensional probabilistic anatomical cranio-cerebral correlation via the international 10-20 system oriented for transcranial functional brain mapping. *NeuroImage.* **21** (1), 99-111 (2004).
41. Herwig, U., Satrapi, P., Schönfeldt-Lecuona, C. Using the international 10-20 EEG system for positioning of transcranial magnetic stimulation. *Brain Topogr.* **16** (2), 95-99 (2003).
42. Indahlastari, A. et al. The importance of accurately representing electrode position in transcranial direct current stimulation computational models. *Brain Stimul.* **16** (3), 930-932 (2023).
43. Woods, A. J., Bryant, V., Sacchetti, D., Gervits, F., Hamilton, R. Effects of electrode drift in transcranial direct current stimulation. *Brain Stimul.* **8** (3), 515-519 (2015).
44. Thair, H., Holloway, A. L., Newport, R., Smith, A. D. Transcranial direct current stimulation (tDCS): A beginner's guide for design and implementation. *Front Neurosci.* **11**, e641 (2017).

45. De Witte, S. et al. Left prefrontal neuronavigated electrode localization in tDCS: 10-20 EEG system versus MRI-guided neuronavigation. *Psychiatry Res Neuroimaging*. **274**, 1-6 (2018).
46. Daoud, M. et al. Stereo-EEG based personalized multichannel transcranial direct current stimulation in drug-resistant epilepsy. *Clin. Neurophysiol*. **137**, 142-151 (2022).
47. Hunold, A., Haueisen, J., Nees, F., Moliadze, V. Review of individualized current flow modeling studies for transcranial electrical stimulation. *J Neurosci Res*. **101** (4), 405-423 (2023).
48. Göksu, C. et al. Human in-vivo brain magnetic resonance current density imaging (MRCDI). *NeuroImage*. **171**, 26-39 (2018).
49. Göksu, C., Scheffler, K., Siebner, H. R., Thielscher, A., Hanson, L. G. The stray magnetic fields in magnetic resonance current density imaging (MRCDI). *EJMP*. **59**, 142-150 (2019).